Baseline Shack Hartmann Design for the 6.5m MMT f/9 Focus

S. C. West (swest@as.arizona.edu) and H. Olson[1]
Multiple Mirror Telescope Observatory, Tucson, AZ

MMTO Technical Memo **#01-01**, September 2001
http://nemo.as.arizona.edu/~swest/pdfs/sh_wfs_tb.pdf (color version)

Abstract

We investigate a Shack Hartmann wavefront sensor for the 6.5m MMT f/9 focus utilizing the original "seeing camera" location within the top box. The model is constructed using the OSLO Premium optical design package. The telescope optics are input, a collimator is chosen to match the pupil size to the detector, and the output of a lenslet array is determined using the OSLO CCL command language written in C. Aberrations are introduced into the system by: 1) miscollimating the secondary mirror and 2) with a Zernike phase surface on the primary mirror. A single representative lenslet is rastered in the pupil of the collimator. The positions of the images formed by the lenslets are determined by tracing the chief ray through each lenslet and solving for the intersection on the detector. Ray aiming through each lenslet is accomplished by constructing a sub-aperture which is the projection of the lenslet onto the entrance pupil. The raw spot displacements are output to another program which then back-calculates the Zernike wavefront. The input and calculated aberrations are compared to check for systematics (discussed in a forth-coming tech memo). The detailed optical model directly shows realistic spot psfs, pupil mapping distortions, and effects due to global wavefront tilts through the lenslet array. Finally, this baseline computation is used as a basis for the selection of the final design.

I. Background

Wavefront analysis at the 6.5m MMT is currently accomplished with a relatively high resolution stand-alone interferometric Hartmann wavefront sensor (described in *MMTO Technical Report* #**37**, 11 June 2001, West, Callahan and Fisher). The intention of this device is to build look-up tables vs. elevation that remove the repeatable components of optical figure distortion and mis-collimation. The idea being that the optical support structure (OSS) is well behaved and that the primary mirror thermal control system will maintain a good optical figure once gravitational effects are removed. Alas, the assumptions are too naive. The difficulties in retro-fitting the existing telescope facility for the substantial off-board thermal control jet ejector system have delayed its implementation even to this date. Additionally, the tangent arms that define the lateral position of the secondary (see e.g. *MMTO Conversion Technical Memo* #**00-0**5, 25 May 2000, West and Allen) degraded causing large and non-repeatable collimation errors. Clearly, this provides a strong indication that the telescope must be operated with *in-situ* wavefront sensors.

A wavefront sensor that utilizes the bare Cassegrain has the advantage of working either with the top box (using the seeing camera position), or attached to a platform connected to the derotator for f/9 instruments that do not use the top box.

A. Optical Design and Results

This is a relatively straightforward design. The beam is slow enough for a simple doublet collimator. The focal length of the collimator is chosen to match the re-imaged entrance pupil to the detector. Here, we design for the 10-mm CCD of an Apogee KX-260 because we already have two of them (512 x 512 with 20-um pixels). The re-imaged pupil size (P) is the ratio of the collimator focal length to the effective f# of the telescope:

$$P = \frac{f_{coll}}{f^{\#}_{tel}} \qquad (1)$$

Thus a collimator of 80mm focal length will deliver a pupil of roughly 9mm diameter.

The as-built telescope optics are input into OSLO. A Zernike phase surface is placed on the primary mirror so we may simulate mirror distortion. The secondary is set up to simulate miscollimation. We put a doublet collimator (MG 01LAO111) spaced by its focal length from the telescope focus. A single lenslet (plano convex) with a 50mm focal length is placed at the pupil formed by the collimator. An OSLO CCL program was written to raster the lenslet within the pupil (appendix A). At each position of the lenslet, rays are aimed through a corresponding sub-aperture stop which is the projection of the lenslet in the entrance pupil. The chief ray is traced through the subaperture, and its intersection with the detector is saved.

1. Now at Colorado State University

Because of the sub-aperture definition, the program calculates spot diagrams, wavefront aberrations, psfs, etc. specific to each lenslet position. This was useful, for example, to verify that the gravitation center of a spot formed by a lenslet near the edge of the pupil was sufficiently close to the chief ray intersection so that the latter was an accurate representation of the spot position.

The worst-case spot and psf occur for lenslets near the edge of the pupil and are shown in Figure 1. The geometric ray trace

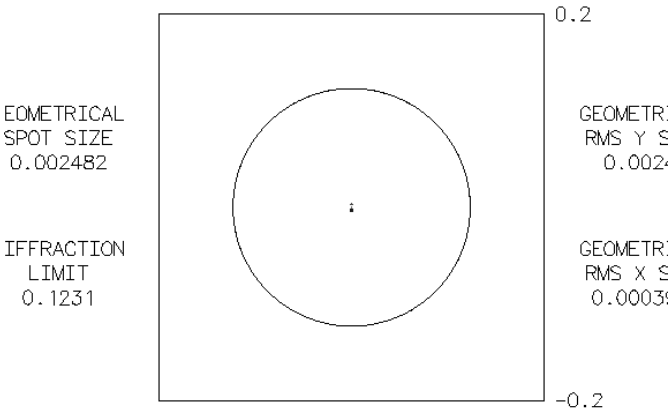

Figure 1: Spot diagram (upper) and psf crossection (lower) produced by a lenslet near the pupil edge. The spot diagram shows the geometric ray trace and the diffraction psf diameter (large circle). The crossection of this psf is shown in the lower diagram. Dimensions are shown in mm.

and the diffraction spot size (D) are shown. The latter's size can be estimated by:

$$D \sim \frac{2.44\lambda}{d_{lenslet}} F_{lenslet} \qquad (2)$$

where d and F are the diameter and focal length of the lenslet. For our case at a wavelength of 800 nm, D is about 200 microns.

The resulting spot pattern on the detector is estimated in Figure 2. This gives 15 samples across the pupil diameter and

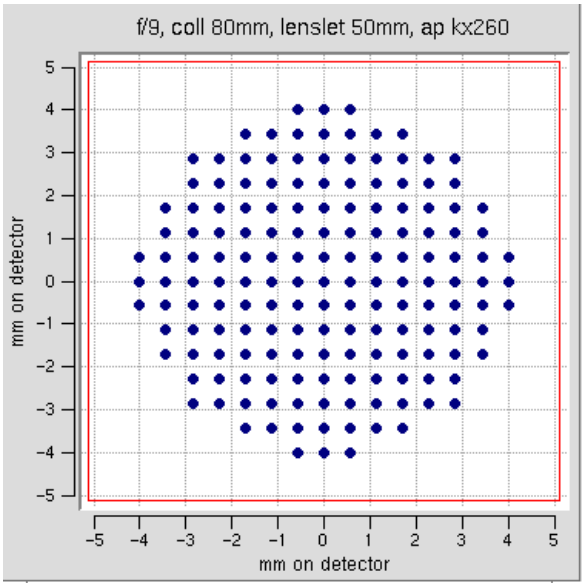

Figure 2: Estimated spot pattern formed by an 80mm collimator and lenslets of diameter 0.5mm with 50mm focal lengths and a 0.57mm pupil spacing. The spot width shown is from Equation 2. The red boundary represents a 512x512 detector with 20 micron pixels.

represents a reasonable trade-off between minimum sampling for lower modes and resolution for diagnostics.

The results of the chief ray traces for several sets of aberrations are shown in the following figures. Each shows the histograms of the x and y spot displacements for the lenslet geometry shown in Figure 2. The wavefront aberrations were produced by changing the orientation of the secondary mirror (M2) and/or inputting wavefront Zernike coefficients onto the primary mirror phase surface. The plots show bins of the spot displacement (microns) on the detector vs. the number of spots in the bin. Figure 3 shows the results for displacing M2. Figure 4 shows the results for a few low order primary mirror Zernike phase distributions.

The spot motion shown in Figure 3 is proportional to the wavefront coefficient and lenslet focal length. In this way, we can estimate the sensitivity for other optical geometries. To

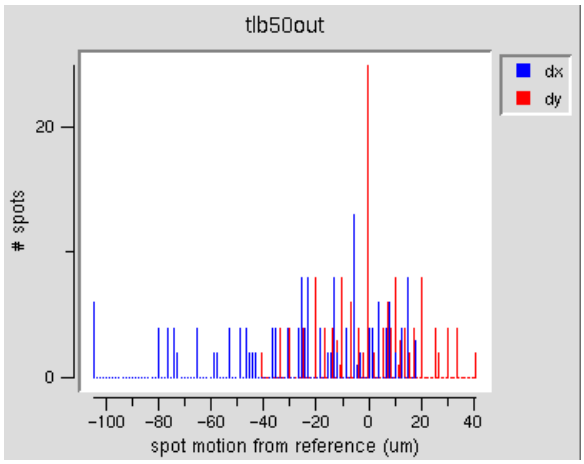

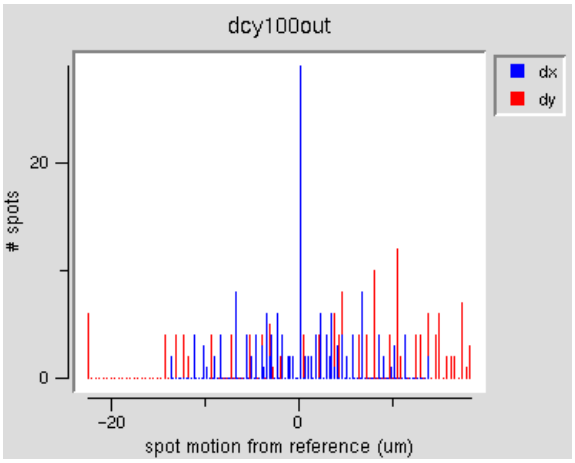

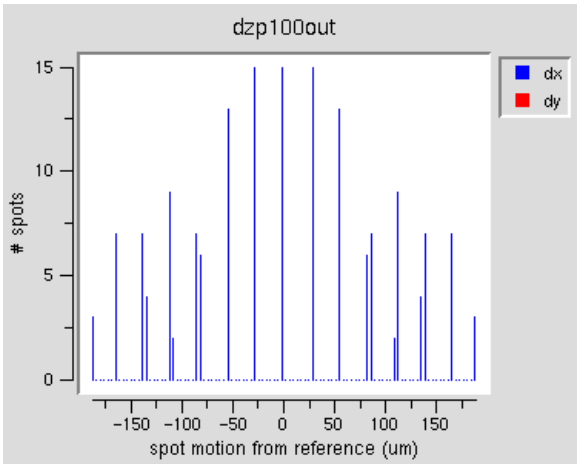

Figure 3: Histograms of x and y spot displacements produced by tilting (top), decentering (middle), and pistoning the secondary mirror (M2). The M2 tilt is 50-arcsec (1450 nm *wavefront* coma), the decenter is 100 microns (500 nm coma), and the piston is 100 um (3800 and 50 nm of wavefront defocus and spherical respectively).

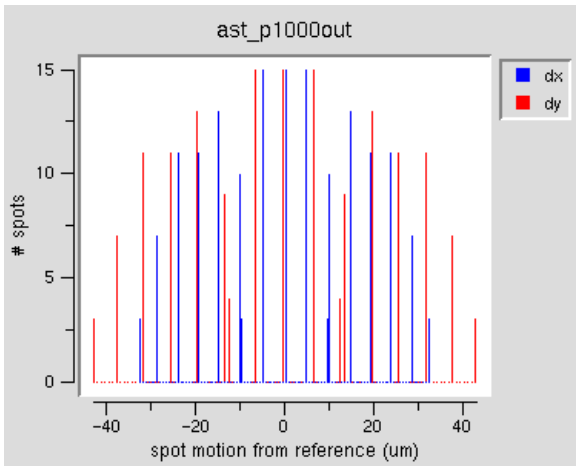

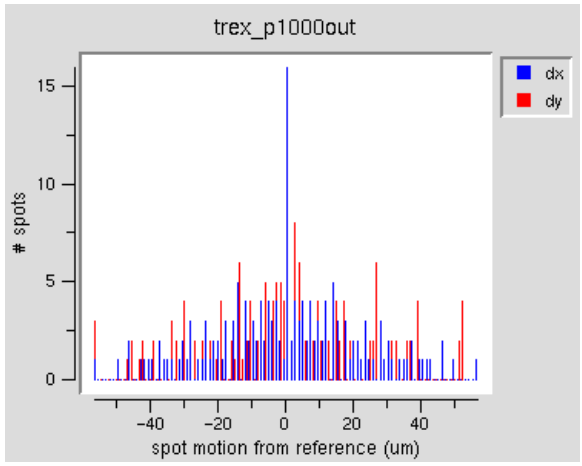

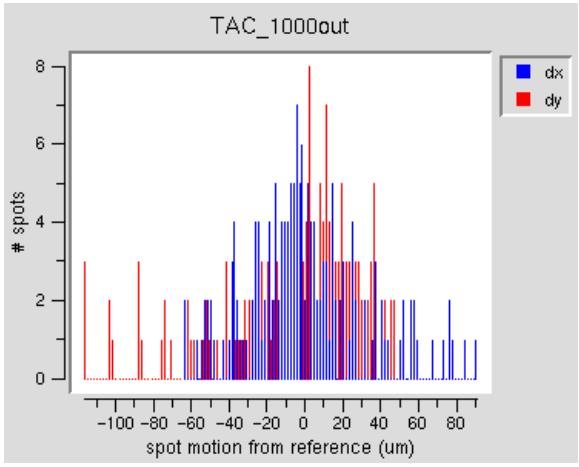

Figure 4: Histograms of x and y spot displacements for low-order mirror bending. From top to bottom are: 1 um of *surface* astigmatism, 1 um of surface 3rd-order trefoil, and a combination of surface astigmatism (1 um), trefoil (1 um), and coma (0.5 um).

help with this scaling, Table 1 show the sensitivity of the

Table 1:

	1um M2 decenter	**1-arcsec M2 vertex tilt**	**1um M1-M2 despace**
coma (nm)	4.98	29.2	--
defocus (nm)	--	--	38.5
spherical (nm)	--	--	0.5

wavefront coefficients for M2 motion that maintains 0.1-arcsec image quality (despace of 7-um: 270nm and 3 nm of defocus and 3rd-order spherical respectively; decenter and vertex tilt of 70 um and 11 arcsec respectively -- ~330 nm of wavefront coma).

The collimator can distort the mapping between the entrance and re-imaged pupils. We investigated this effect with our model by comparing the position of the chief ray on the detector with the ideal position of the lenslet in the re-imaged pupil (Figure 5).

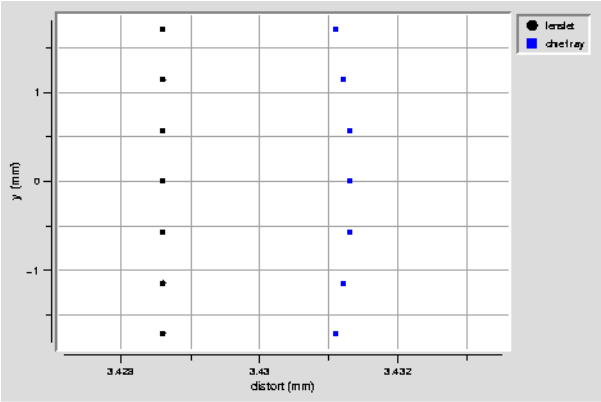

Figure 5: An estimate of the mapping distortion created by the collimator (and lenslets) plotted at the detector. The ideal column of spots shown (black) are from Figure 2 (3rd column from the right). The mapping distortion is shown by the blue spots. It is at most about 2 microns which corresponds to about 1.5mm on the primary mirror.

A C program was written to fit a Zernike wavefront to the spot displacements output by the OSLO CCL script. Although OSLO is capable of solving for the Zernike fit to aberrations present in the design, it manipulates the reference wavefront sphere to remove tilt and defocus. Additionally, it can't account for any systematic effects produced by a measurement of the wavefront derived from the discrete lenslet array. The method used here of back-calculating Zernikes from the output of lenslets includes most all effects one could expect from the actual device. The results of this back calculation will be discussed in another memo.

II. Conclusions

We made a guess at a Shack Hartmann design for the f/9 Cassegrain focus of the 6.5m MMT consisting of an 80mm doublet collimator and 50mm lenslets. The design was thoroughly investigated with a model and CCL script using OSLO.

The ray trace and psf for the worst case lenslets at the edge of the pupil (Figure 1) and the small mapping distortion (Figure 5) show that the commercial doublet collimator performs well. The diffraction from 0.5mm diameter lenslets and pupil sampling we chose would work well on a 10mm detector.

However, it's evident from Figures 3 and 4 that the 50mm lenslet focal length provides barely enough spot displacement to easily measure our ultimate optical specifications for the telescope (see e.g. MMTO Technical Report #35 Dec. 1999), Fabricant, McLeod, and West: see also the end of MMTO Technical Report #28 June 1995), West and Martin). However, as the bottom of Figure 4 shows, this lenslet focal length provides about the right amount of sensitivity for the magnitude of aberrations we typically see without primary mirror thermal control (MMTO Technical Report #37, June 2001).

The main problem with a longer lenslet focal length is the size of the diffraction spot. For example, with the pupil sampling geometry used here, the diffraction pattern of adjacent spots overlap for a lenslet focal length of 100mm. Less pupil sampling and larger diameter lenslets would make a 150mm lenslet focal length possible, and we think that would provide good sensitivity for a fully tuned telescope working at its specifications.

Our proposal for an f/9 Shack Hartmann wavefront sensor is two fold. Substitute a 75mm lenslet focal length into this baseline design to be used for the checkout period after summer shutdown 2001 while the thermal control and modifications to the M2 support system are ongoing. The tolerance to large aberrations and the spatial sampling this model gives will be very useful during this period. The 75mm focal length will increase spot displacements (and spot size) shown here by 50%. Once these systems are performing at their design levels, we purpose substituting at least a 150mm lenslet and either reduce the pupil sampling and increase the lenslet diameter to fit the 10mm detector, or determine another geometry with a larger CCD and re-imaged pupil.

After checking the Adaptive Optics website (www.aoainc.com), the selection of standard arrays is not as diverse as we'd like. The tooling charge for a custom array appears to be ~$12K with no educational discount. Standard

arrays cost ~$1K. The following standard arrays come closest to meeting our needs and can be replicated on BK7 substrates.

Table 2: Adaptive Optics Associates standard arrays that provide the best matches for our geometry.

pitch (um)	focal length (mm)	format	aperture
625	45	13 x 13	hex
500	45	14 x 14	square
1000	55	25 x 25	square
1000	45	9 x 9	hex
768	86	32 x 32	square

The delivery time is about 1 month. Figure 6 illustrates the fit

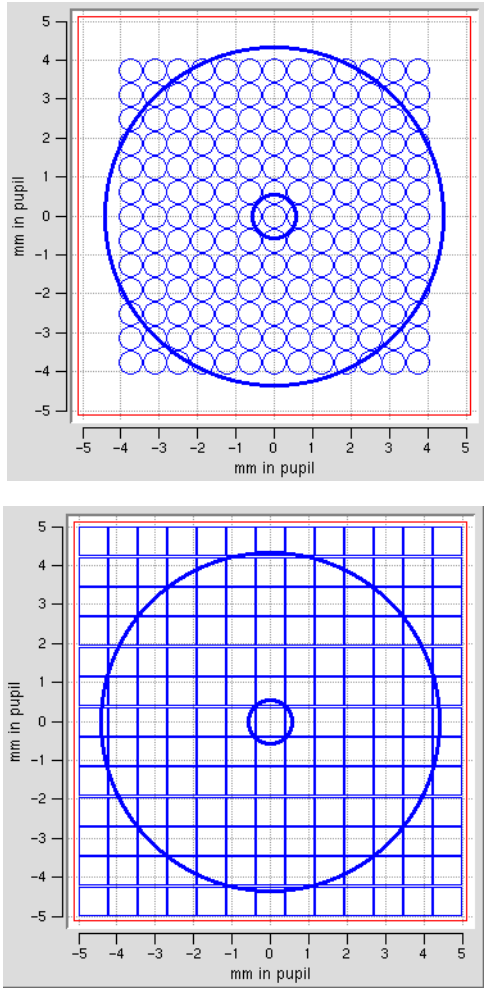

Figure 6: Pupil plane geometry for two standard arrays from Table 2. The top is the 625-45-H (hex apertures approximated with circles) and the 768-86-S.

of two standard lenslet arrays superimposed on the re-imaged pupil.

III. Appendix A (OSLO CCL)

/* CCL for calculating the spot positions of a lenslet
 * array. Place the MMT and SHartmann into the
 * spreadsheet. This program rasters a single lenslet
 * in the pupil plane while moving the corresponding
 * projection of the lenslet in the entrance aperture.
 * It then finds the position of the chief ray through
 * each lenslet on the detector (i.e. the ideal spot
"* position). User sets up M2 offsets and object params
"*as needed for each desired case, then runs this script
"*for each case. */

```
cmd lenslet(void)
{
        float E2P = 731.30384; /* pupil demagnification */
        int outfp, xyfp, i, j, end;
        real k,l,x,y;
        float xc[500],yc[500];
        char line[1000], xs, ys;

        outfp = fopen("TAC_1000out", w);
        if (outfp <=0)
                {printf ("outfp is %d\n", outfp);
                fclose (outfp); return;}
        xyfp = fopen("xy",r);
        printf ("file pointer is %d\n", xyfp);

        /* read in the xy lenslet array coords (mm at pupil)
          remember to remove octave comments from file */

        i = 0;
        end=1;
        while (end >=0)
        {
                 end = fscanf (xyfp, "%f %f\n", &x, &y );
                 xc[i] = x; yc[i] = y; /* scanf didn't like &xc[i] */
                 printf ("line %d contains %f %f\n", i, x,y);
                i++;
        }
        fclose (xyfp);
        printf ("Lines in file are %d\n", i); /* max index is i-1 */

        set_preference(output_text, on);
        /* set up reference wavefront
         * the lenslet is decentered on surf 12
         * the sub-entrance aperture is on surf 1
         * M2 is adjusted on surf 4 by user. */

        dcy 1 0; dcx 1 0; /* clear subaperture decenters */
        dcy 12 0; dcx 12 0; /* clear lenslet decenters */
        /* sop 0 0 0; /* set object point to axis */

        for (j=0;j<i-1;j++)
        {
                dcx 12 xc[j]; dcy 12 yc[j]; /* decenter lenslet */
                dcx 1 -1*xc[j]*E2P; dcy 1 -1*yc[j]*E2P; /* decenter entrance ap */
                ssbuf_reset();

                trr;/* trace chief ray */
                /* print xy coords from spreadsheet buffer to file */
                fprintf (outfp,"%10.4f %10.4f\n",b3, a3);
        }

        fclose (outfp);
        /* clear ast and lenslet decenters */
        dcy 1 0 ; dcx 1 0;
        dcy 12 0; dcx 12 0;
}
```